The Influence of Uniform Flow on Tropical Cyclone Intensity Change

JOEY H. Y. KWOK AND JOHNNY C. L. CHAN*

Laboratory for Atmospheric Research
Department of Physics and Materials Science, City University of Hong Kong

Submitted to
Journal of the Atmospheric Sciences

Revised
October 2004

**Corresponding Author Address*: Johnny Chan, Department of Physics and Materials Science, City University of Hong Kong, Tat Chee Avenue, Kowloon, Hong Kong, China. Email: Johnny.chan@cityu.edu.hk

ABSTRACT

The influence of a uniform flow on the structural changes of a tropical cyclone (TC) is investigated using the Pennsylvania State University/National Center for Atmospheric Research Mesoscale Model Version 5 (MM5). Idealized experiments are performed on either an *f* plane or a beta plane. A strong uniform flow on an *f* plane results in a weaker vortex due to the development of a vertical wind shear induced by the asymmetric vertical motion, and a rotation of the upper-level anticyclone. The asymmetric vertical motion also reduces the secondary circulation of the vortex.

On a beta plane with no flow, a broad anticyclonic flow is found to the southeast of the vortex, which expands with time. Similar to the *f*-plane case, asymmetric vertical motion and vertical wind shear are also found. This beta-induced shear weakens the no-flow case significantly relative to that on an *f*-plane. When a uniform flow is imposed on a beta plane, an easterly flow produces a stronger asymmetry whereas a westerly flow reduces it. In addition, an easterly uniform flow tends to strengthen the beta-induced shear whereas a westerly flow appears to reduce it by altering the magnitude and direction of the shear vector. As a result, a westerly flow enhances TC development while an easterly flow reduces it.

The vortex tilt and mid-level warming found in this study agree with previous investigations of vertical wind shear. A strong uniform flow with a constant *f* results in a tilted and deformed potential vorticity at the upper levels. For a variable *f*, such tilting is more pronounced for a vortex in an easterly flow, while a westerly flow reduces the tilt. In addition, the vortex tilt appears to be related to the mid-level warming such that the warm core in the lower troposphere cannot extend upward, which leads to the subsequent weakening of the TC.

1. Introduction

In recent years, significant research efforts have been devoted to studying the intensity change of tropical cyclones (TCs), most of which focused on interactions between the TC and its environment. For example, Challa and Pfeffer (1980) examined the eddy flux of angular momentum using a numerical model and found that TCs with a larger eddy flux convergence of angular momentum near the sea level are more likely to intensify. In terms of the upper-level outflow structure, Ooyama (1987) showed in a numerical simulation that asymmetric outflow patterns could be generated in the presence of horizontal shear. He suggested that the evolution of hurricane outflow is important to both TC motion and structural change. Based on a composite study, Merrill (1988) concluded that an intensifying hurricane typically had an extended upper-level outflow channel while a non-intensifying hurricane usually had a unidirectional flow over the center.

The effect of environmental vertical wind shear on TC intensity change has also been studied extensively in recent years (e.g. Jones 1995, 2000a, b; DeMaria 1996; Bender 1997; Frank and Ritchie 1999, 2001; Ritchie 2004). Potential vorticity asymmetries near the eyewall region have been attributed as causes of a vortex tilt downshear of the TC and the subsequent weakening.

While these complicated processes have been extensively studied, the effect of a uniform flow on TC intensity change is still unclear even in an *f*-plane situation. For example, Frank and Ritchie (2001) found that a TC in a 3.5 m s^{-1} uniform background flow slightly intensifies compared with a no-flow case. They attributed this result to the more favorable boundary layer conditions for the moving storm; the resultant advection of warm air is found in part of the eyewall, where it develops a higher equivalent potential temperature region. However, in an earlier modeling study, Peng et al. (1999) showed that a TC weakens in a uniform flow of 5-10 m s^{-1}. They concluded that a mean flow induces the vortex asymmetry

through surface friction, and a phase difference exists between the asymmetric moisture convergence and surface flux, which reduces precipitation and causes TC weakening. In a similar study, Dengler and Keyser (2000, hereafter DK2000) found that a region of convectively stable air is formed to the left of the uniform flow vector. This convectively stable air penetrated into regions of boundary layer convergence, which reduces vortex intensity.

For a variable *f*, both Peng et al. (1999) and DK2000 showed that a westerly flow is more favorable for storm intensification than an easterly flow. However, Peng et al. (1999) shows that the maximum intensity of a vortex under a westerly flow is stronger than that of the no-flow case, which appears to be opposite to the result of DK2000.

Such discrepancies suggested that the mechanisms that affect TC intensity under a uniform flow have not been clearly identified. Therefore, it is necessary to re-examine TC structure and intensity changes in the simplest case of a uniform flow on an *f* plane as well as a beta plane, which is the objective of the present study.

Section 2 describes the model configurations and the generation of the bogus vortex. The intensity changes of the vortices are shown in section 3. Wong and Chan (2004, hereafter WC04) have pointed out that asymmetric flow patterns and vertical motion are associated with the vertical wind shear and the subsequent weakening of TC. Section 4 therefore attempts to compare such asymmetries for different vortices. These results lead to the conclusion that vertical winds shear is induced by the uniform flow, so that the evolution, magnitudes and directions of which will be presented in section 5. Mid-level warming and vortex tilt previously discussed by DeMaria (1996) and WC04 are presented in section 6. Finally, concluding remarks are given in section 7.

2. Model configuration and bogus vortex

a. Model configuration

The Pennsylvania State University/National Center for Atmospheric Research Mesoscale Model Version 5 (MM5) is used in this study. The model domain consists of 301 x 301 grid points with a grid size of 15 km and 24 full sigma (σ) levels. The Coriolis parameter (f) is set constant at 20º N for f-plane experiments. For variable f, the initial locations of vortices are centered at 20º N. The model top is set at 50 hPa, and the reference sea-level pressure at 1010 hPa. The terrain height is set to zero, and the vegetation category is set to water bodies everywhere. The vertical temperature gradient is proportional to $\log p$ below 100 hPa and is kept constant above 100 hPa. The sea-surface temperature is kept unchanged at 28.5 ºC. The relative humidity profile decreases linearly from 80% near surface to 10% at 300 hPa and above. Boundary layer processes are determined from the Eta (Mellor-Yamada) scheme (Janjić 1990, 1994).

The simple ice-explicit moisture scheme (Dudhia 1989) and the Betts-Miller cumulus parameterization scheme (version without explicit downdraft) (Betts and Miller 1986) are used to spin up the vortex for the first 24 h. The Betts-Miller scheme is then switched off, and the remaining 72 h simulations are performed using the explicit moisture scheme. Atmospheric radiation, multi-layer soil temperature and shallow convection have been turned off in all the experiments.

b. Bogus vortex

All experiments are initialized with the same axisymmetric, baroclinic vortex. The maximum wind of the vortex is initially 30 m s^{-1} at a radius of 70 km. The radius of 15 m s^{-1} wind is at 400 km. This bogus vortex has 985 hPa as its minimum sea-level pressure.

The horizontal wind field $V_T(r)$ is defined according to Chan and Williams's (1987) horizontal wind profile:

$$V_T(r) = V_{\max}\left(\frac{r}{r_{\max}}\right)\exp\left\{\frac{1}{b}\left[1-\left(\frac{r}{r_{\max}}\right)^b\right]\right\},$$

where r is the radius, $r_{\max}$ the radius of maximum wind and $V_{\max}$ the maximum wind. The parameter b represents the size of the bogus TC and b = 0.33 in all simulated TCs in this study. A vertical structure is introduced to the horizontal wind field by multiplying $V_T(r)$ by a function $w(p)$ that decreases monotonically with pressure above 850 hPa:

$$w(p) = \left[\frac{3(p/p_m)}{2+(p/p_m)^3}\right]$$

where p_m is the vertical level of maximum tangential wind, which is set at 850 hPa. Temperatures are calculated by thermal wind balance, pressure perturbations are computed from the hypsometric equation, and geopotential heights are set according to gradient balance.

The bogus TC is then spun up on an *f* plane for 24 h of model time. Its intensity after spun up is 970 hPa, with a symmetric flow at 850 hPa (Fig. 1a), a broad anticyclone with clear outflow at 200 hPa (Fig. 1b). The tangential wind (Fig. 1c) and radial wind (Fig. 1d) distributions at this time remain highly symmetric.

The effect of mean flow and planetary vorticity gradient (beta) are studied by comparing 2 groups of experiments (see Table 1): Group *f* consists of 4 sets of *f*-plane simulations with zonal uniform flow strengths of 0, 4, 6 and 8 m s^{-1}. Group beta consists of 5 sets of beta-plane simulations with zonal uniform flow strengths of -8, -4, 0, 4 and 8 m s^{-1}. All the imposed wind fields in this study are horizontally uniform at all sigma levels. For simplicity, all the TCs in the current study are named as their respective experimental codes in Table 1.

3. Intensity of vortices

a. Vortices on an f plane

Comparing the cases within group *f* indicates that a uniform flow suppresses TC intensification (Fig. 2a). A vortex with no flow (the fu[0] case) is the strongest in all the experiments. It intensifies gradually from 975 hPa to 916 hPa by 51 h, and then it slightly weakens to 920 hPa until the end of model time. The TC under a relatively weak (4 m s^{-1}) uniform flow (the fu[4] case) has its intensity changes very similar to that of the fu[0] case in the first 36 h. Its rate of intensification then decreases slightly relative to the no-flow case between t = 36 and 57 h, and its intensity is kept at ~920 hPa towards the end. When a stronger uniform flow is imposed, the rate of intensification decreases, with the intensities of the cases fu[6] and fu[8] leveling off at t = 21 and 24 h respectively. At t = 72 h, the respective minimum sea-level pressures of experiments fu[6] and fu[8] are 946 and 954 hPa. Therefore, with a constant *f*, a stronger uniform flow results in a larger intensity reduction of the vortex. On the other hand, a weak mean flow (4 m s^{-1}) reduces the intensification rate of a TC but its maximum intensity is unchanged, which appears to agree the results of with Peng et al. (1999) (see their Fig. 1a).

b. Vortices with variable f

The intensity evolution of vortices for group beta (variable *f*) depends on the direction of the imposed uniform flow. A TC on an *f* plane without background flow (fu[0]) intensifies much quicker than its beta-plane counterpart (bu[0]) (cf. Fig. 2a and 2b), with the latter reaching a maximum intensity of 947 hPa at t = 72 h, which is 27 hPa higher than that in the fu[0] case. This result that the beta effect reduces the intensification rate of a TC as well as its maximum intensity, is consistent with those from some previous studies (e.g. DeMaria and Schubert 1984; Peng et al. 1999).

When a uniform flow is imposed to a TC on a beta plane, the results appear to be partly consistent with those from previous studies (Peng et al. 1999; DK2000), i.e. westerlies are more favorable for TC intensification than easterlies (Fig. 2b). In fact, the stronger the westerly flow, the more the TC intensifies on a beta plane (i.e. bu[8] > bu[4] > bu[0]). However, Peng et al. (1999) shows that only weak westerly flows (3-5 m s^{-1}) are favorable for TC intensification, and any stronger mean flow does not help the vortex to intensify. For the easterly flow cases, the bu(-4) vortex stops deepening after 12 h of intensification, with its intensity being 959 hPa at t = 72 h. The weakest vortex in this group is the bu[-8] case. It stopped intensifying after t = 12 h, and further weakens from t = 24 h – 36 h, having an intensity of 967 hPa at t = 72 h.

These results suggest that either a strong mean flow or the planetary vorticity gradient (beta) can reduce the intensity of a TC. Further, vortex intensification on a beta plane depends on the direction of the applied uniform flow: a westerly flow enhances intensification while an easterly flow reduces it, and this effect is more prominent with a stronger uniform flow. The rest of this paper will focus on the following experiments: fu[0], fu[8], bu[-8], bu[0] and bu[8], because a stronger uniform flow appears to have a larger effect to their intensity changes.

Based on these results and those of previous studies, the following working hypothesis may be formulated: A uniform flow produces an asymmetry in the vortex, and when the asymmetry in vertical motion is strong enough, it weakens the secondary circulation of the TC as described by WC04 (see their Fig. 13 for details), which leads to the development of vertical wind shear. This shear results in the subsequent vortex tilt and mid-level warming so that the intensity of the vortex is reduced. The next few sections will attempt to validate such a hypothesis.

4. Asymmetric vertical motion and flow patterns

Previous studies have demonstrated that asymmetric structures should produce a negative impact on TC intensification (Bender 1997; Peng et al. 1999; Frank and Ritchie 2001). WC04 suggested that subsidence in the eyewall region is formed by asymmetric vertical motion, which develops a temperature asymmetry by the entrainment of cooler air to the upper TC core. In that way, vortex tilt and mid-level warming occur so that the TC is weakened. In other words, vertical motion asymmetries play an important role in the evolution of the secondary circulation of the vortex. In the current study, the vertical motion of different cases are investigated at $\sigma = 0.525$.

a. Vortices on an f plane

The control vortex (the fu[0] case) has the most symmetric vertical motion. Strong rising motion is found at the eyewall region, and weak sinking motion (< 0.5 m s^{-1}) is found outside the eyewall (example shown for t = 48 h, Fig. 3). For the vortex with an 8 m s^{-1} flow, a wavenumber-1 asymmetry in vertical velocity is found in the fu[8] case as early as at t = 3 h (Fig. 4a). As the vortex intensifies until t = 36 h, rising motion near the eyewall increases, with a prominent wavenumber-1 vertical motion asymmetry of strong rising motion from the northeast to southwest, and maximum sinking motion (~1.5 m s^{-1}) is found to the southwest (Fig. 4b). As discussed in WC04, vertical wind shear is associated with the sinking motion near the eyewall, which results in the subsequent reduction of secondary circulation and the intensity of vortex. Therefore, the asymmetry in vertical motion observed here may be related to the development of a vertical wind shear, which will be discussed in section 5. The vertical motion is still asymmetric at t = 72 h (Fig. 4c). The magnitude of rising motion has decreased and the sinking motion is not as strong as in t = 36 h, probably because the vortex does not further weaken from t = 36 to 72 h.

Large-scale flow asymmetries in the upper troposphere are similar to those found by WC04. While the 850-hPa flow for the fu[8] case remains largely symmetric and cyclonic at t = 36 and 72 h (Figs. 5b, d), anticyclonic flow is found at 200 hPa, at 400 km to the east of the vortex center at t = 36 h (Fig. 5a). As the vortex keeps moving eastward at 8 m s^{-1}, the anticyclone rotates southwestward relative to the TC and is located 600 km to the south of the vortex center by t = 72 h (Fig. 5c). The sheared cases in Wu and Emanuel (1994) and WC04 also showed a similar movement of the anticyclone relative to the vortex center. WC04 further showed that changes in the direction and magnitude of the vertical wind shear are accompanied with such rotation of the anticyclone, which will be discussed in section 5.

To summarize, a uniform flow with constant *f* produces a wavenumber-1 asymmetry in vertical motion, which leads to subsidence at the eyewall. In other words, the secondary circulation is reduced on part of the vortex. Establishment of an anticyclone at 200 hPa and its subsequent rotation apparently leads to a vertical wind shear over the TC.

b. Vortices with variable f

Asymmetric vertical motion can be found in all the cases on a beta plane. For the bu[0] case, the vortex at t = 3 h shows a fairly symmetric vertical motion (Fig. 6a), because the beta effect has not taken place at such an early stage. By 36 h, the beta effect is fully established so that a wavenumber-1 asymmetric vertical motion is developed, with rising motion mainly found to the east and strong sinking motion to the north of the eyewall (Fig. 6b). Such a wavenumber-1 vertical motion asymmetry remains at t = 72 h, with rising motion being prominent to the south, and sinking motion is stronger to the north (Fig. 6c).

In both the easterly (bu[-8]) and westerly flow (bu[8]) cases, a wavenumber-1 asymmetric vertical motion is already present after 3 h of model time (Figs. 7a , 8a). Note that at t = 3 h, the asymmetry in the bu[8] case is similar to that in the fu[8] case (see Fig. 4a),

because the beta effect has not developed. After 36 h of integration, the easterly flow case shows a small area of strong rising motion in the southeastern part of the eyewall (Fig. 7b). On the other hand, the rising motion for its westerly flow counterpart is more prominent to the northwest and southeast, which shows a wavenumber-2 asymmetry (Fig. 8b). This difference in vertical motion is more significant at t = 72h. For the bu[-8] case (Fig. 7c), vertical motion at $\sigma = 0.525$ is highly asymmetric with rising motion mainly to the north, while the vertical motion of the bu[8] case is more symmetric than bu[-8] (Fig. 8c).

The influence of beta effect to the changes in circulation has been extensively studied in TC motion (e.g. Chan and Williams 1987). An initially axisymmetric TC on a beta plane is found to propagate northwestward, which is basically induced by the beta gyres that create a northwestward ventilation flow through self-advective processes.

As expected, for the zero mean flow case on a beta plane (i.e. the bu[0] case), an 850-hPa anticyclonic flow is first developed to the east of the vortex at t = 36 h (Fig. 9b), producing a wavenumber-1 flow pattern. This pattern maintains in quasi-steady state and the anticyclone expands with time. The anticyclone at 850 hPa shifted slightly to the north at t = 72 h (Fig. 9d). At 200 hPa, anticyclonic flow is first developed to the north of the vortex at t = 36 h (Fig. 9a). It then rotates in a clockwise direction so that by 72 h it is to the southwest of the vortex (Fig. 9c). Such a rotation therefore induces a vertical wind shear and hence the subsequent vertical motion asymmetry, as discussed in WC04.

When a strong easterly flow (the bu[-8] case) is imposed, no significant changes are found in the 850-hPa flow, with anticyclonic flow to its east and southeast at both 36 h and 72 h (Figs. 10b and d respectively). Note, however, that the cyclonic circulation of the bu[-8] vortex is smaller than that of the bu[0] vortex, probably as a result of the strong easterly flow. For the 200-hPa flow, anticyclonic flow is found to the southeast of the vortex at t = 36 h (Fig. 10a). The flow at t = 72 h is highly asymmetric, with two large anticyclones to the northeast

and southwest of the vortex (Fig. 10c). For the bu[-8] case, the flow appears to be near-barotropic to the southeast of the vortex, with anticyclonic flow at both the 850 and 200-hPa levels (Fig. 11). Not much rotation is observed from t = 36 to t = 72 h.

To summarize, vortices are in general more asymmetric on a beta plane than on an *f* plane. The beta gyres induce a wavenumber-1 asymmetry to the vertical motion and such asymmetry strengthens with time. Subsequent weakening of vertical motion on one side of the vortex also appears to reduce the secondary circulation. An easterly uniform flow imposed on a beta plane enhances the vertical motion asymmetry while a westerly flow reduces it, so that a more symmetric secondary circulation is found in the latter. For all the cases on a beta plane, the 850-hPa anticyclone is generally maintained in a quasi-steady state to the southeast of the vortex but the upper anticyclone appears to rotate relative to the vortex center except for the bu[8] case, so that the orientation of the 200-850 hPa vertical wind shear appears to vary with time.

Ritchie (2004) pointed out that the direction of the vertical wind shear is induced on a beta plane and is at an arbitrary angle to the motion vector. In the next section, the relationship between intensity change and vertical wind shear evolutions in these cases are investigated.

5. Vertical wind shear

The vertical wind shear between the upper (200 hPa) and lower (850 hPa) levels is computed following WC04: the zonal and meridional winds at 200 and 850 hPa are interpolated onto a 15 km × 5º azimuth polar grid relative to the vortex center. Area averaging of the 200-850 hPa shear is then performed on a 450 km disc. WC04 found that most of the temporal variations of the shear occur near the core (i.e. 0-400 km). Therefore, shears beyond the 450-km radius will not be discussed.

Consistent with the results of WC04, the core shears for the fu[0] case stay below 2 m s^{-1} (Fig. 12a). For the fu[8] case, the core shear quickly develops and reaches a 8 m s^{-1} crest at t = 27 h (Fig. 12a), which is associated with the asymmetric vertical motion (see Fig. 4b in section 4a). The strong shear apparently weakens the secondary circulation through subsidence. Southwesterly shear is found prior to t = 30 h but the direction changes to southeasterly afterwards (Figs. 13, 15), which is consistent with the flow patterns shown in Fig. 5.

On a beta plane, the total shear magnitudes for the 3 cases generally follow the order: bu[-8] > bu[0] > bu[8] (Fig. 12b), which basically agrees with the asymmetric vertical motion found in section 4a as well as our hypothesis that a stronger vertical motion asymmetry is associated with a stronger vertical wind shear. As for the direction of shear, northwesterly shear is found for the bu[0] case (Figs. 14, 15). Under a strong easterly flow (the bu[-8] case), the northerly shear generally increases first (Figs. 14b, 15), followed by an increase in westerly shear towards the end of the simulation (Figs. 14a, 15). In the westerly flow (bu[8]) case, the shear changes from weak easterly (Figs. 14a, 15) to weak northwesterly (Fig. 14b, 15). In other words, the vertical shear associated with a westerly uniform flow on a beta plane opposes the direction of the beta-induced shear whereas that of an easterly uniform flow strengthens it.

The vector plot in Fig. 15 illustrates that a northwesterly shear is generally found in the cases on a beta plane, but an easterly/southeasterly shear is found in the fu[8] case. Note that between t = 30 and 48 h, the shear vectors of bu[0] and fu[8] are almost completely opposite to each other, and the superposition of these two shear vectors give approximately the shear vector bu[8]. Of course, such a direct superposition will not reveal the true bu[8] case. Nevertheless, these results suggest that the shear induced by a westerly uniform flow

indeed opposes the beta-induced shear, which leads to a reduction of shear in bu[8] relative to bu[0].

6. Vortex tilt and temperature anomaly

DeMaria (1996) and WC04 have demonstrated that vertical wind shear may cause a vortex tilt, which is probably one of the major mechanisms for TC weakening. DeMaria (1996) also found that the tilted potential vorticity (PV) pattern is associated with an increased mid-level warming near the TC core, which may reduce convective activity and inhibit TC development. In the present study, the PV of the fu[8] case tilts downshear to the north at t = 36 h (Fig. 16a, b), and the tilt is more prominent at t = 72 h, where upper-level PV is ~100 km to the west (Fig. 16c) and ~60 km to the south (Fig. 16d) of the vortex center. This vortex tilt agrees with the southeasterly shear orientation discussed in section 5 (see Fig. 15).

Among all the simulations on the beta plane, bu[-8] has the most prominent vortex tilt. At t = 36 h, the zonal PV is tilted downshear (Fig. 17a) while the meridional PV is tilted slightly upshear (Fig. 17b). The PV at t = 72 h shows that the vortex is tilted downshear, and the strong vertical PV cannot extent upward into the outflow layer. Such a weak upper-level PV implies a weak upper-level circulation and hence a weak TC. The weak core shear in the bu[8] case naturally does not produce much tilt of the vortex (Fig. 18) and thus bu[8] has the highest intensity among the vortices in group beta.

Mid-level warming associated with the PV tilt as described by DeMaria (1996) and WC04 is also found in this study. As in WC04, temperatures at each σ level are interpolated onto a 15-km × 5º azimuth polar grid centered on the TC surface center, and the temperature anomaly is defined as the temperature within a 60-km radius averaged vortex core relative to that in a quiescent state.

The fu[8] case shows an increased temperature anomaly (~1.5 K) in the mid-lower troposphere whereas its upper-level core temperature is ~6 K lower than that in the fu[0] case (Fig. 18a). In other words, the fu[8] vortex is tilted such that warming of the core cannot extend to the upper-troposphere through diabatic heating.

On a beta-plane, the bu[0] case also shows a mid-level warming relative to the fu[0] case (Fig. 19b). When the temperature anomalies of the 3 beta-plane cases are compared, the easterly flow case (fu[-8]) shows a prominent mid-level warming (~2 K) with a reduced upper-level core temperature (~4.5 K) relative to the no-flow case (bu[0], Fig. 19c), whereas the westerly flow case (fu[8]) has a warmer core relative to the no-flow case (Fig. 19d). In this way, the strength of diabatic heating for these vortices appears to be in the order: bu[8] > bu[0] > bu[-8], which is consistent with their intensity changes.

To summarize, vortex tilt and mid-level warming occur subsequent to the establishment of vertical wind shear. When a uniform flow is imposed on an *f* plane, the asymmetry-induced vertical wind shear leads to a downshear tilt of the vortex. Mid-level warming associated with a weaker upper-level temperature anomaly is found relative to the control vortex (the fu[0] case).

On a beta plane, an easterly flow increases the beta-induced shear and thus enhances its vortex tilt and the related mid-level warming. Reduction of the beta-induced shear is found in the westerly-flow case so that very little vortex tilt is observed, and the core is warmer relative to the no-flow case on a beta plane. Such a warm core appears to be the consequence of an increased diabatic heating, which results in a higher intensity relative to the no-flow case.

7. Concluding remarks

In the real atmosphere, tropical cyclones (TCs) seldom exist in a constant uniform background flow. However, idealized modeling provides insights of the interactions between the uniform flow and the TC so that the structural and intensity changes in such a quasi-steady environment can be examined.

In this study, the effects of a uniform flow on both *f* plane and beta plane have been examined. A strong uniform flow imposed on an *f* plane results in a weaker vortex, which is due to the development of vertical wind shear induced by an asymmetry in vertical motion. Wavenumber-1 asymmetries in vertical motion and a rotation of the upper-level anticyclone appear to reduce the secondary circulation of the vortex, which introduces a vertical wind shear. The induced vertical wind shear further weakens the secondary circulation of the vortex as described by WC04 so that the vortex under a strong uniform flow weakens with time. For a weak uniform flow, the asymmetric vertical motion is not strong enough to reduce the secondary circulation so that vertical wind shear cannot develop.

The no-flow case on a beta plane is weakened significantly by the beta-induced shear relative to that on an *f* plane. A westerly uniform flow enhances TC development by canceling part of the beta-induced shear whereas an easterly flow strengthens it by altering the magnitude and direction of the shear vector.

Vortex tilt and mid-level warming found in this study agrees with previous investigations on vertical wind shear. A strong uniform flow on an *f* plane results in a tilted and deformed potential vorticity at the upper levels. On a beta plane, such tilting is more pronounced for a vortex under an easterly flow, while a westerly flow reduces the tilt. In addition, mid-level warming and the subsequent TC weakening are related to the vortex tilt and the magnitude of the shear, which is consistent with the results of DeMaria (1996) and WC04.

Previous studies suggest that a uniform flow on an *f* plane only has trivial effects on TC intensity changes. Some of these claimed that a uniform flow weakens the TC (e.g. Peng et al 1999) while the others found intensification (e.g. Frank and Ritchie 2001), and their intensity changes compared with the no-flow case is typically small. Results of this study suggest that a uniform flow with constant *f* can induce an appreciable vertical wind shear if the uniform flow is strong enough. The beta-induced shear described by Ritchie (2004) is also found in this study, with a westerly uniform flow reducing the shear while an easterly flow enhances it.

If a strong uniform flow induces a vertical wind shear by generating asymmetries in the horizontal TC structure, a horizontal wind shear would alter this asymmetry in a different way, which could result in a different vertical wind shear profile. Thus, the effect of horizontal wind shear on the TC structure and intensity changes should be examined. As TC intensity changes have also been shown to be sensitive to a varying sea-surface temperatures, the effect of this together with the uniform flow should also be examined in future studies.

Acknowledgments. The authors would like to thank Mr. Martin Wong for helpful discussions. Comments from the reviewers have helped in significant improvements of the paper and are gratefully acknowledged. This research is sponsored by the Research Grant Council of the Hong Kong Special Administrative Region, China Grant CityU 1050/02P.

References

Bender, M. A., 1997: The effect of relative flow on the asymmetric structure if the interior of hurricanes. *J. Atmos. Sci.,* **54**, 703-724.

Betts, A.K. and M. J. Miller, 1986: A new convective adjustment scheme. Part II: A new convective adjustment scheme, Part II: Single column tests using GATE wave, BOMEX, ATEX and arctic air-mass data sets. *Quart. J. Roy. Meteor. Soc.*, **112,** 693-709.

Challa, M., and R. L. Pfeffer, 1980: Effects of eddy fluxes of angular momentum on model hurricane development. J. *Atmos. Sci.*, **37**, 1603-1618.

Chan, J. C. L., and R. T. Williams, 1987: Analytical and numerical studies of the beta-effect in tropical cyclone motion. Part I: Zero mean flow. *J. Atmos. Sci*., **44**, 1257-1265.

DeMaria, M., and W. H. Schubert, 1984: Experiments with a spectral tropical cyclone model. *J. Atmos. Sci.* **41**, 901-924.

DeMaria, M., 1996: The effect of vertical shear on tropical cyclone intensity change. *J. Atmos. Sci.*, **53**, 2076-2087.

Dengler, K., and D. Keyser, 2000: Intensification of tropical-cyclone-like vortices in uniform zonal background-flows. *Quart. J. Roy. Meteor. Soc.*, **126,** 549-568.

Dudhia, J., 1989: Numerical study of convection observed during the winter monsoon experiment using a mesoscale two-dimensional model, *J. Atmos. Sci.*, **46**, 3077-3107.

Frank, W. M., and E. A. Ritchie, 1999: Effects of environmental flow upon tropical cyclone structure. *Mon Wea. Rev.*, **127,** 2044-2061.

Frank, W. M., and E. A. Ritchie, 2001: Effects of vertical wind shear on the intensity and structure of numerically simulated hurricanes. *Mon. Wea. Rev.*, **129,** 2249-2269.

Janjić, Z.I., 1990: Step-mountain coordinate, physical package. *Mon. Wea. Rev.,* **118**, 1249-1443.

Janjić, Z.I., 1994: Step-mountain Eta coordinate model: Further developments of the convection, viscous sublayer, and turbulence closure schemes. *Mon. Wea. Rev.,* **122**, 927-945.

Jones, S. C., 1995: The evolution of vortices in vertical shear. Part I: Initially barotropic vortices. *Quart. J. Roy. Meteor. Soc.*, **121,** 821-851.

Jones, S. C., 2000a: The evolution of vortices in vertical shear. II: Large-scale asymmetries. *Quart. J. Roy. Meteor. Soc.*, **126,** 3137-3159.

Jones, S. C., 2000b: The evolution of vortices in vertical shear. III: Baroclinic vortices. *Quart. J. Roy. Meteor. Soc.*, **126,** 3161-3185.

Merrill, R. T., 1988: Environmental influences on hurricane intensification. *J. Atmos. Sci*., **45,** 1678-1687.

Ooyama, K. V., 1987: Numerical experiments of steady and transient jets with a simple model of the hurricanes outflow layer. *Preprints*, *17th Conf. on Hurricanes and Tropical Meteorology,* Miami, FL, Amer. Meteor. Soc., 318-320.

Peng, M. S., B. F. Jeng, and R. T. Williams, 1999: A numerical study on tropical cyclone intensification. Part I: Beta effect and mean flow effect. *J. Atmos. Sci.*, **56,** 1404-1423.

Ritchie, E. A., 2004: Tropical cyclones in complex vertical shears. *Preprints, 26th Conf. on Hurricanes and Tropical Meteorology,* Miami, FL, Amer. Meteor. Soc., 88-89.

Wong, M. L. M. and J. C. L. Chan, 2004: Tropical cyclone intensity in vertical wind shear. *J. Atmos. Sci.*, **61,** 1859-1876.

Wu, C. C., and Emanuel, K. A. 1993: Interaction of a baroclinic vortex with background shear: Application to hurricane movement. *J. Atmos. Sci.,* **50**, 62-76.

Wu, C. C., and Emanuel, K. A. 1994: On hurricane outflow structure. *J. Atmos. Sci.*, **51**, 1995-2004.

List of Figures

Fig. 13. 0 - 450 km area-averaged (a) zonal, (b) meridional vertical wind shear (200 - 850 hPa, unit: m s^{-1}) for group f experiments.

Fig. 14. As in Fig. 13 except for the group beta experiments.

Fig. 15. Time evolution of the vector shear for the fu[8], bu[0], bu[8] and bu[-8] cases respectively.

Fig. 16. Vertical potential vorticity variations (unit: PVU) in (a),(c) zonal component, and (b),(d) meridional component for the fu[8] case, values larger than 8 PVU are shaded. (Contour intervals: 2)

Fig. 17. As in Fig.16 except for the bu[-8] case.

Fig. 18. As in Fig. 16 except for the bu[8] case, values larger than 18 PVU are shaded (contour interval: 2).

Fig. 19. Time-height cross-section of temperature anomalies with a radius of 60 km from the vortex center (unit: K) for (a) fu[8] and (b) bu[0] cases relative to that of fu[0], and (c) bu[-8], and (d) bu[8] cases relative to that of bu[0]. Positive values are shaded. (Contour interval: 0.5)

List of Tables

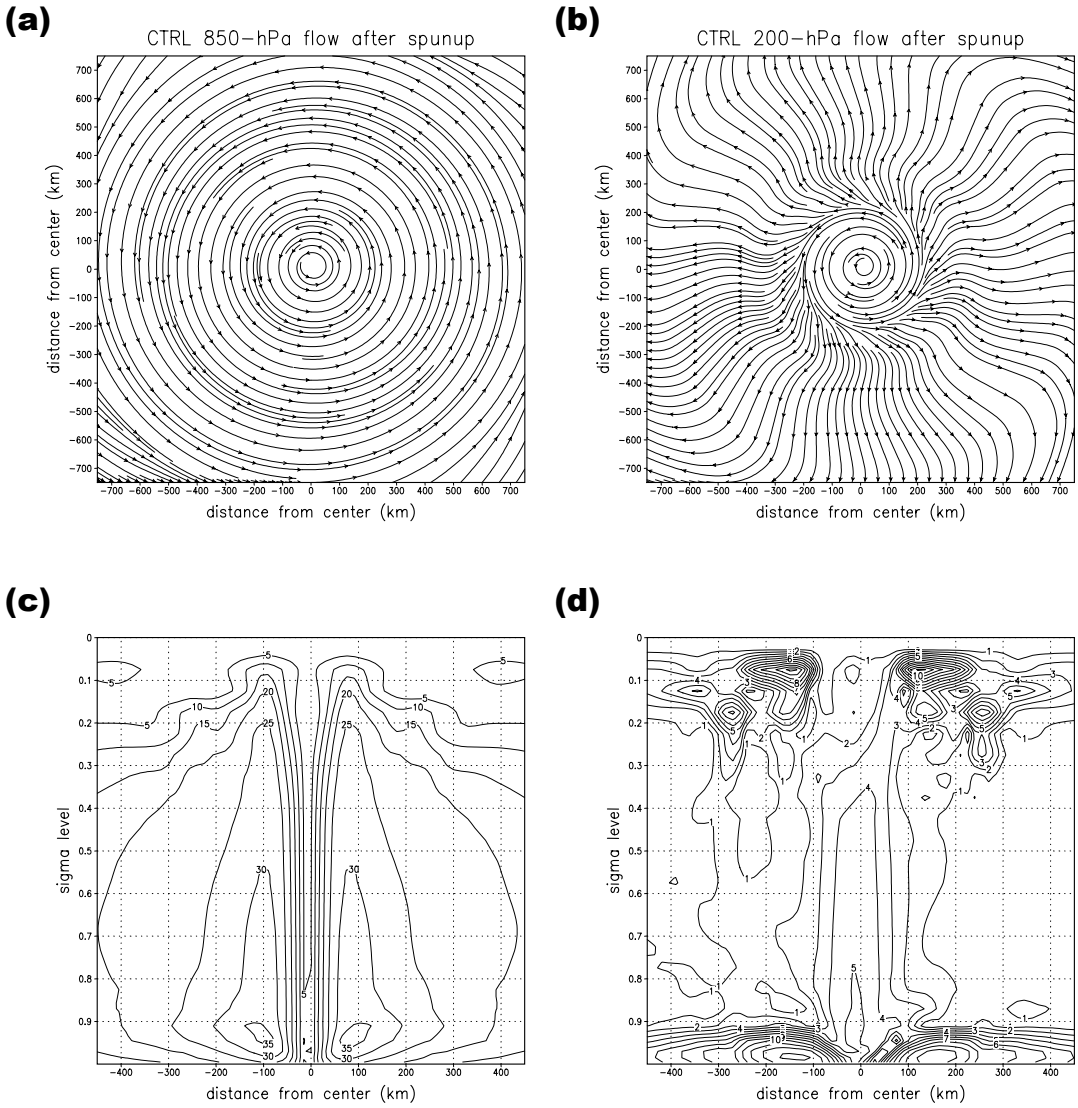

Fig. 1: (a) 850 hPa and (b) 200 hPa streamlines, and (c) tangential (unit: m s^{-1}, contour interval: 5) and (d) radial wind distributions (unit: m s^{-1}, contour interval: 1) after the initial vortex has been spun up for 24 h.

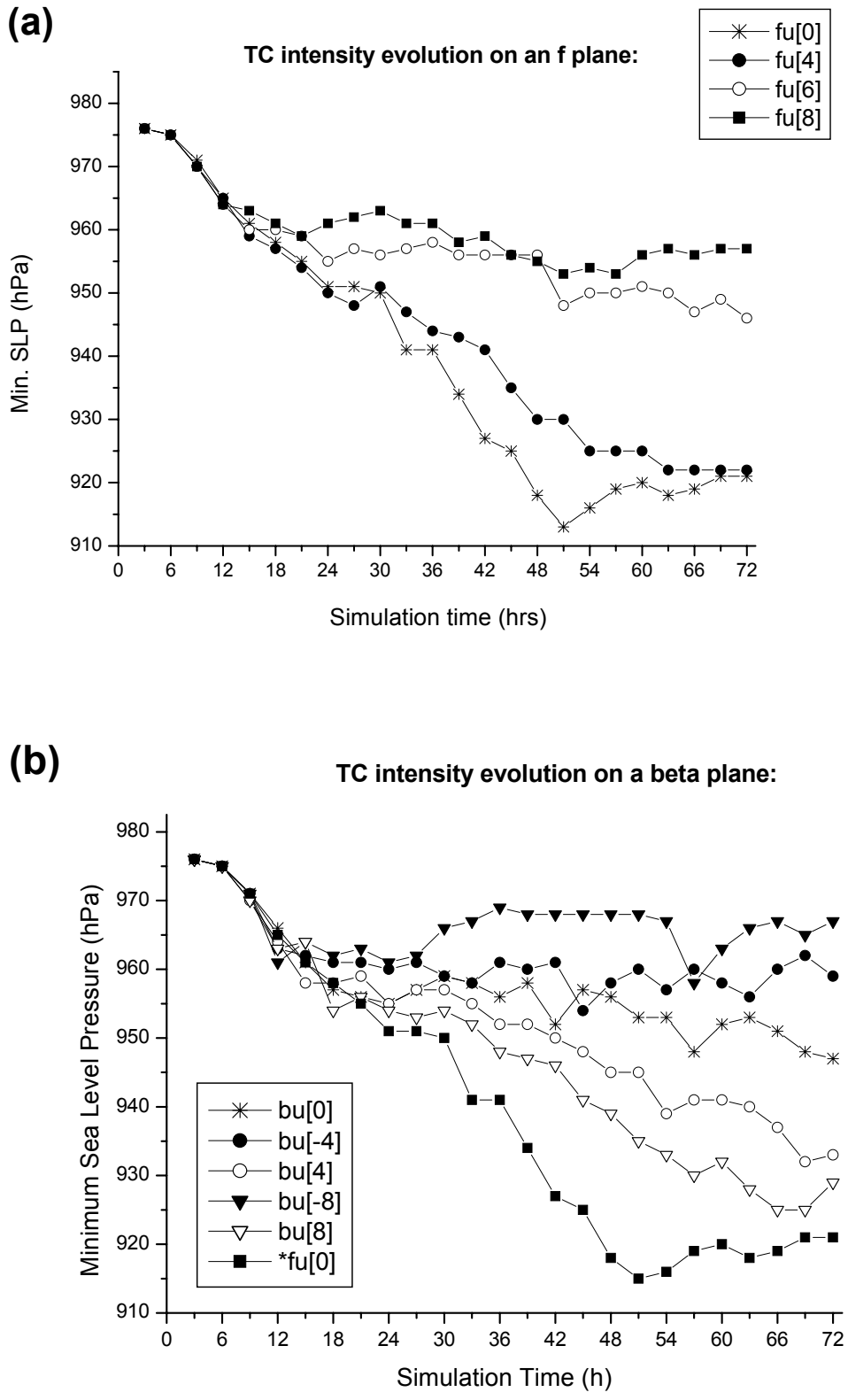

Fig. 2: Intensity evolution of vortices in (a) group f (constant *f*) and (b) group beta (variable *f*, *fu[0] is shown for easy comparison).

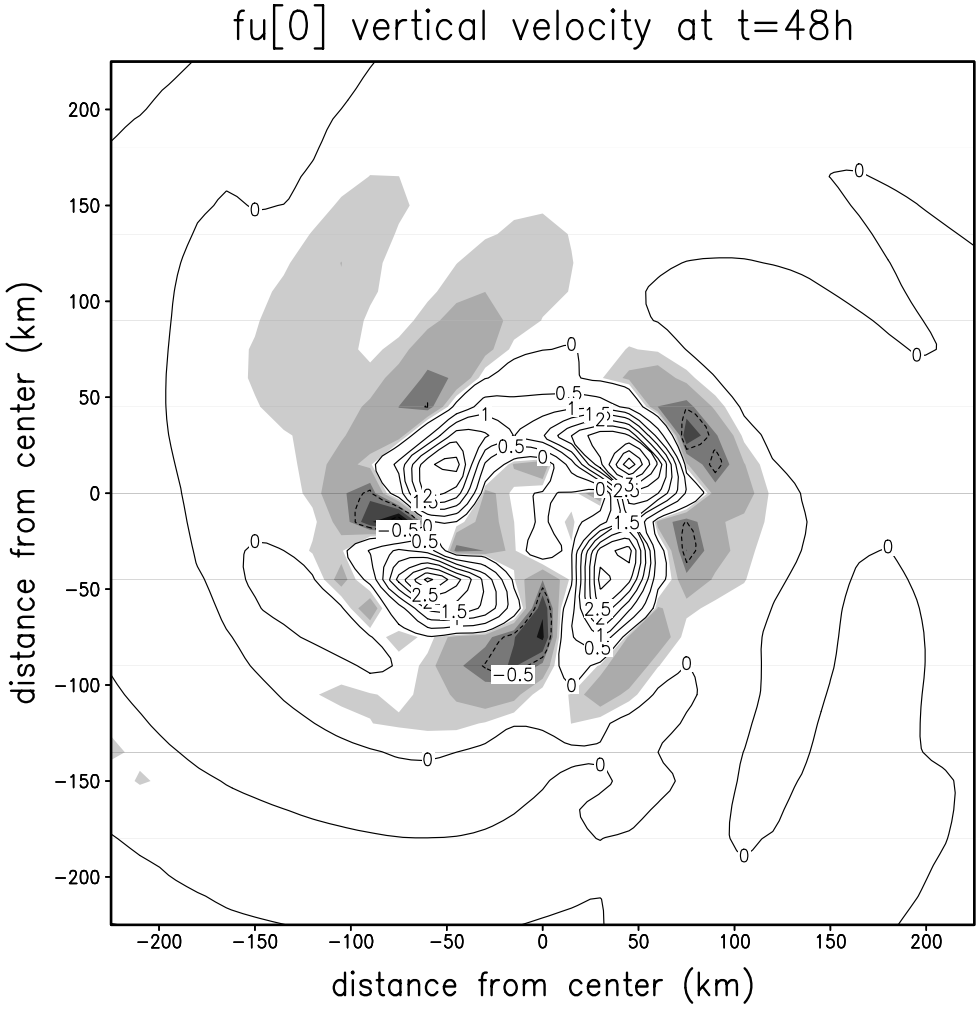

Fig. 3: Vertical motion (unit: m s^{-1}, contour interval: 0.5) at sigma = 0.525 for the control vortex (fu[0]) at t = 48 h, negative values (sinking motion) are shaded.

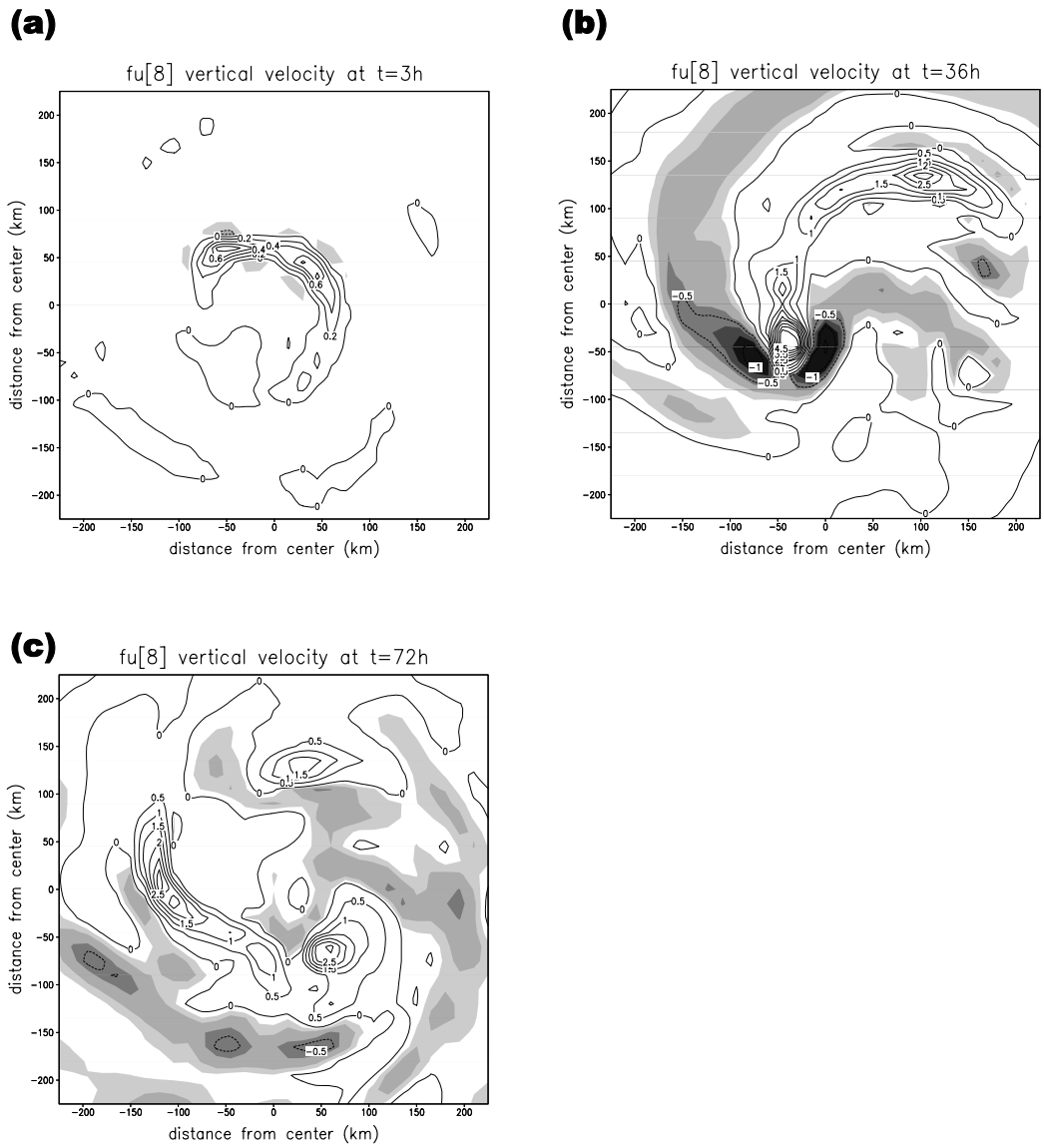

Fig. 4: Vertical motion (unit: m s^{-1}) at sigma = 0.525 for the vortex under 8 m s^{-1} uniform flow (fu[8]) at (a) t = 3 h, (b) t = 36 h and (c) t = 72 h (contour interval: 0.5 for (a), 0.2 for (b) and (c)), negative values (sinking motion) are shaded.

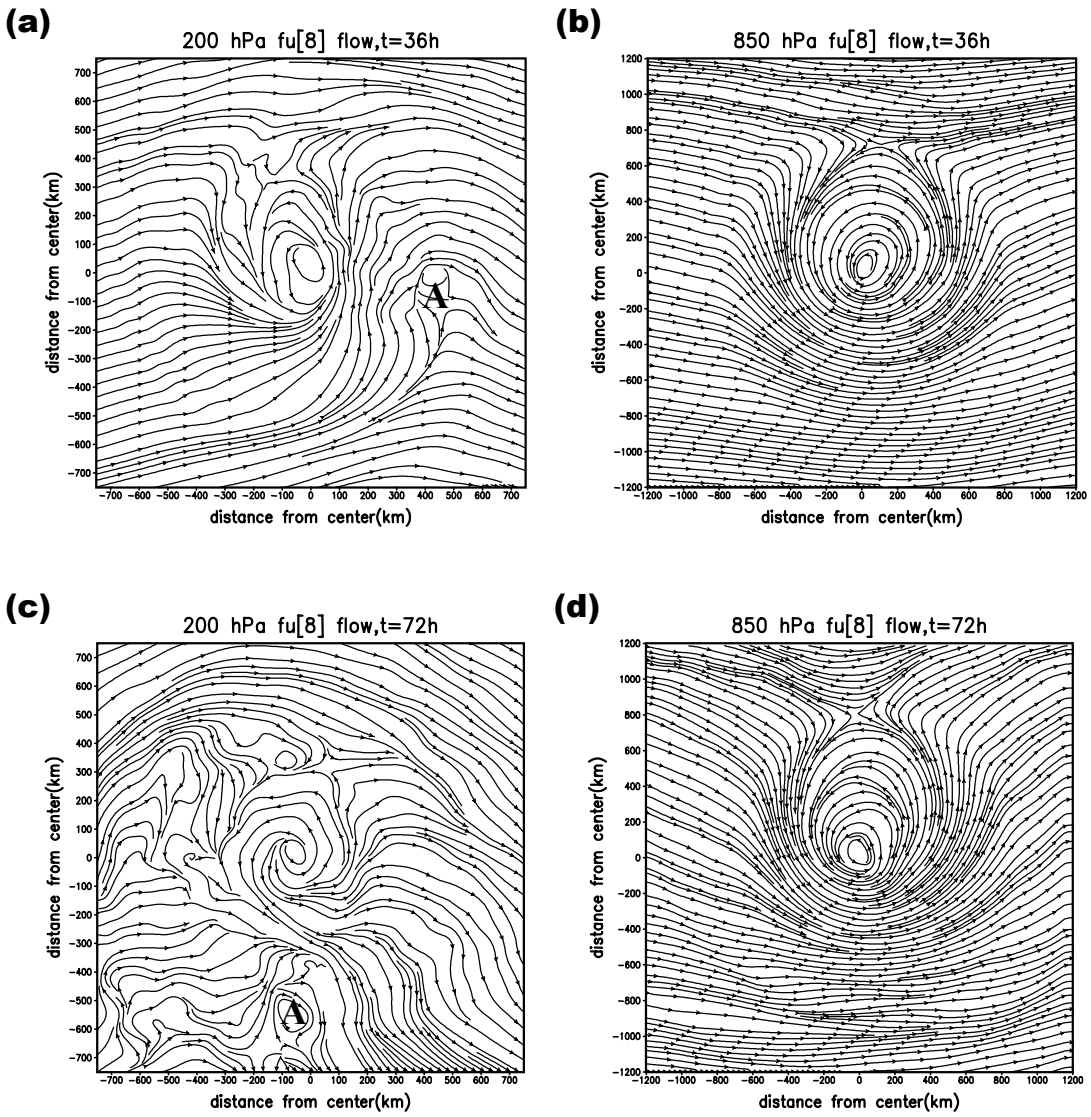

Fig. 5: (a), (c) 200-hPa and (b), (d) 850-hPa streamline plots at t = 36 h and 72 h respectively for the fu[8] case. In (a) and (c), "A" denotes the location of the major anticyclone.

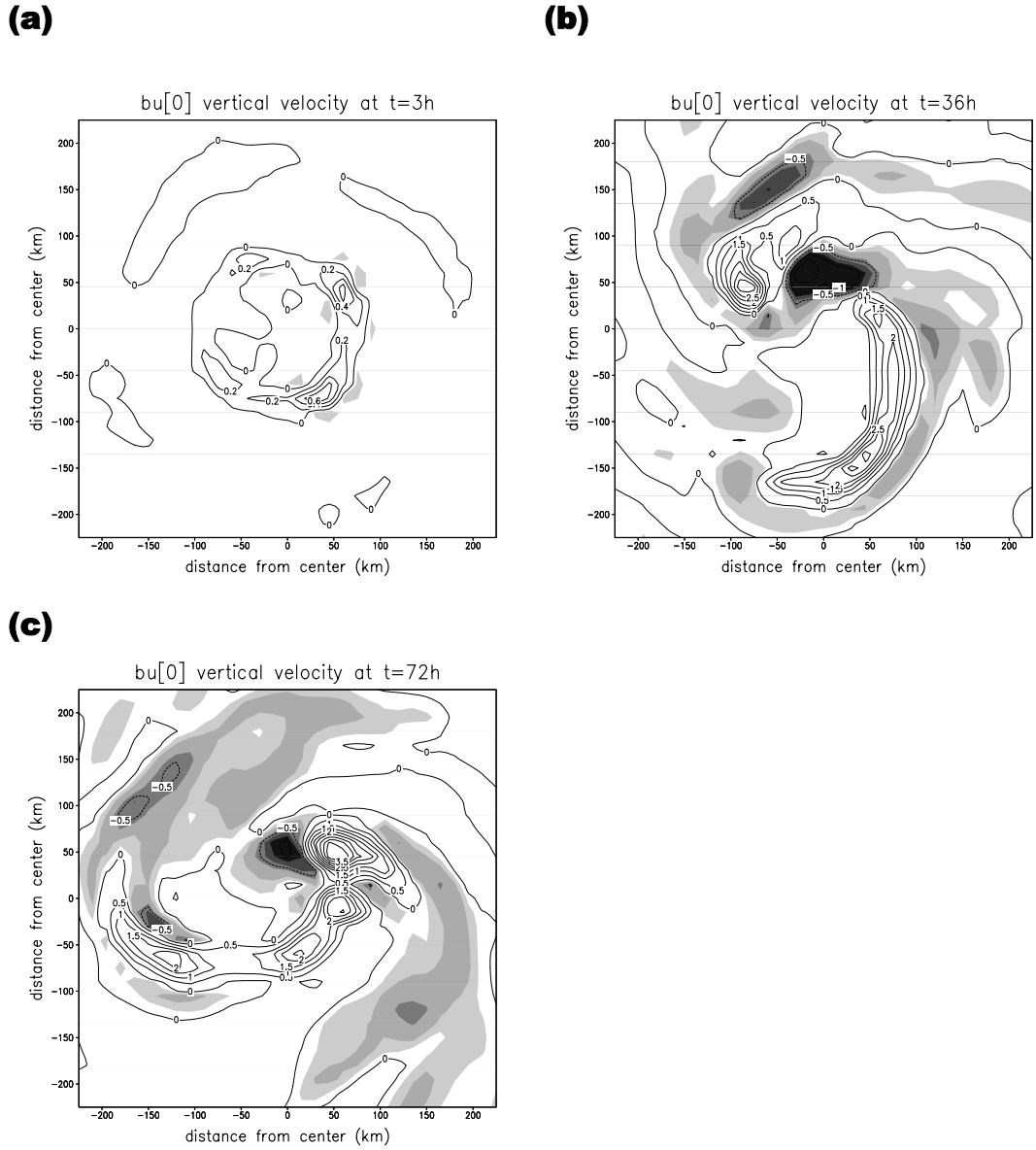

Fig. 6: As in Fig. 4 except for the vortex on a beta plane without a background flow (bu[0]).

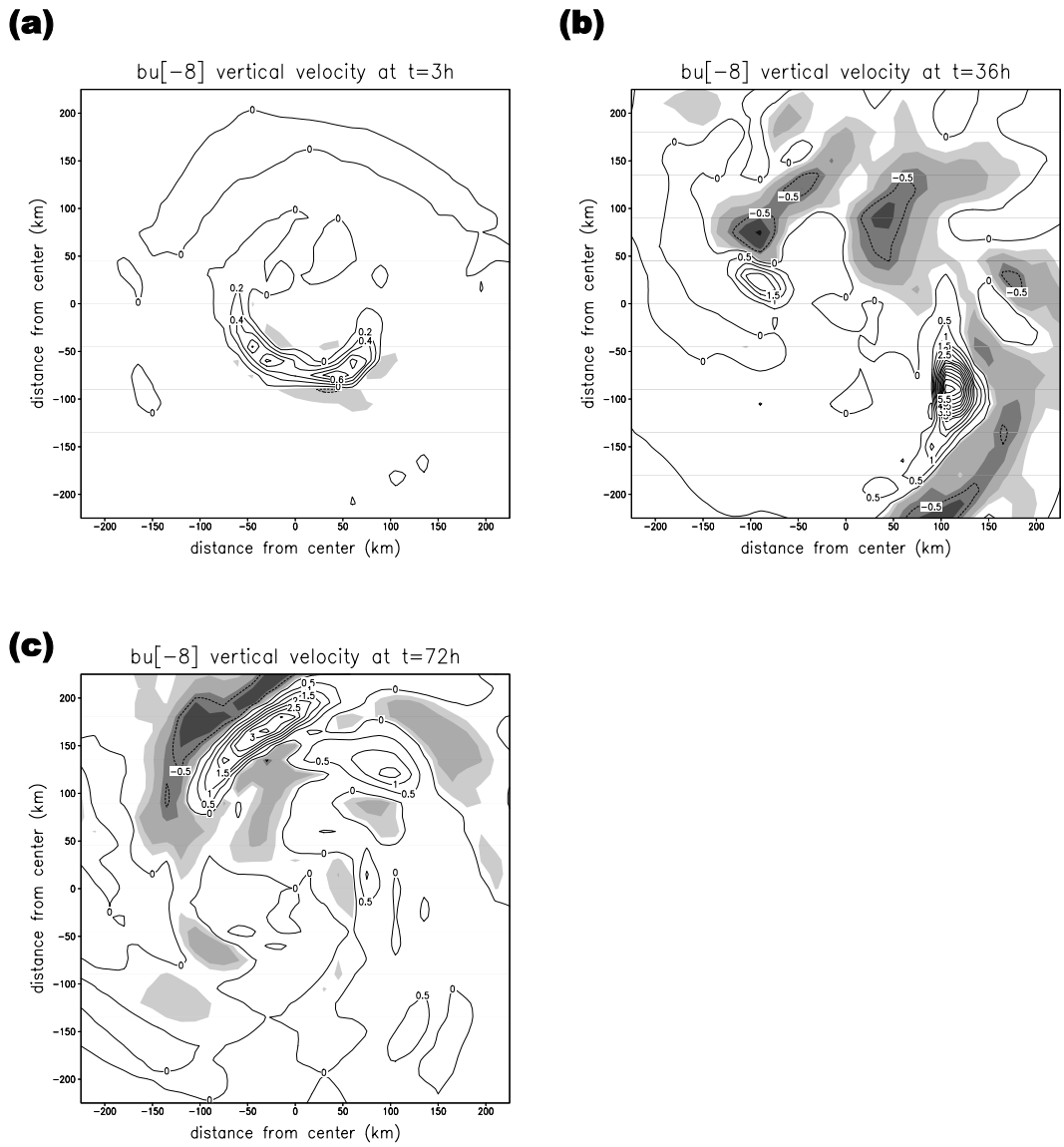

Fig. 7: As in Fig. 4 except for the vortex under a 8 m s^{-1} easterly flow on a beta plane (bu[-8]).

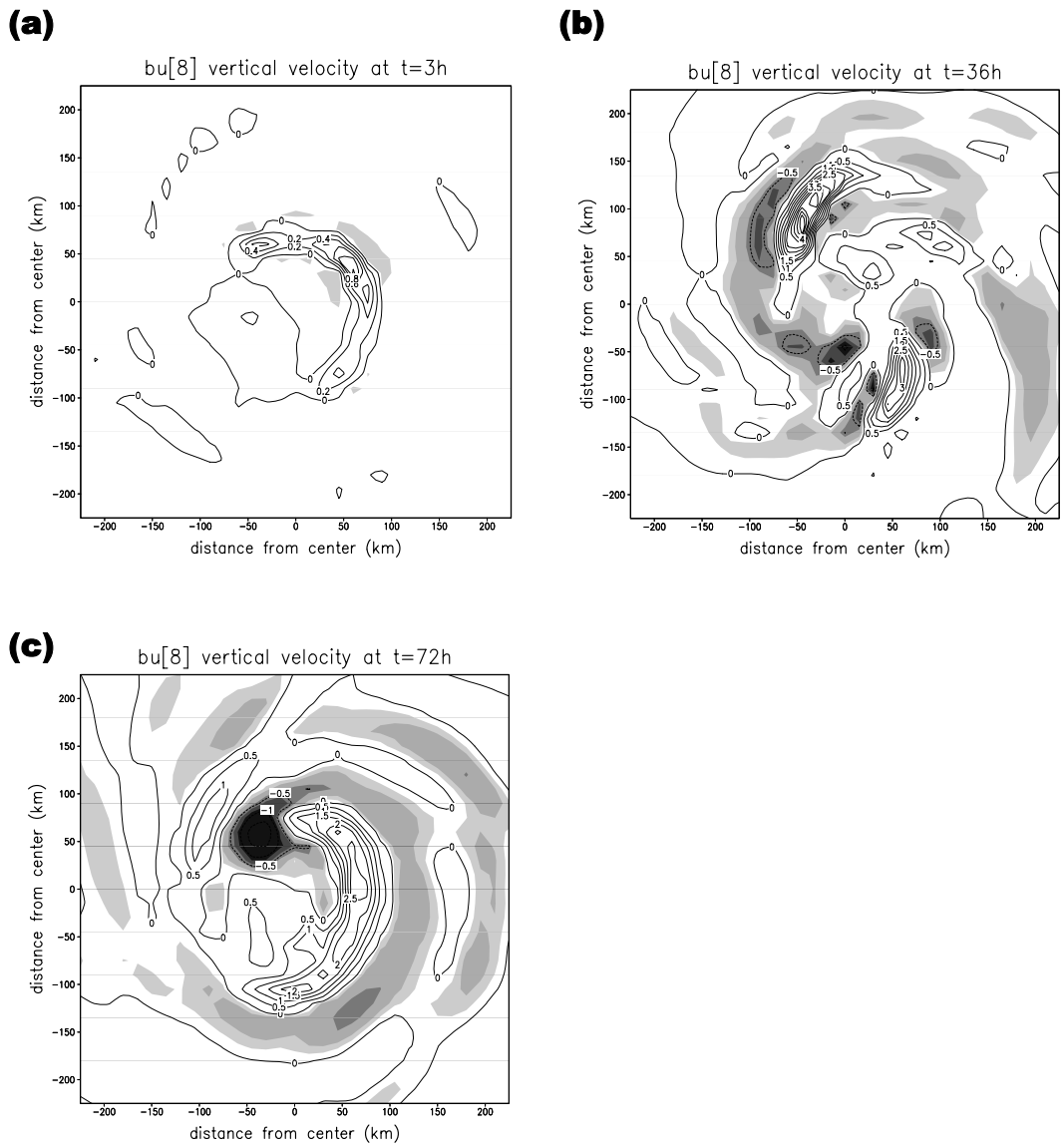

Fig. 8: As in Fig. 4 except for the vortex under a 8 m s^{-1} westerly flow on a beta plane. (bu[8]).

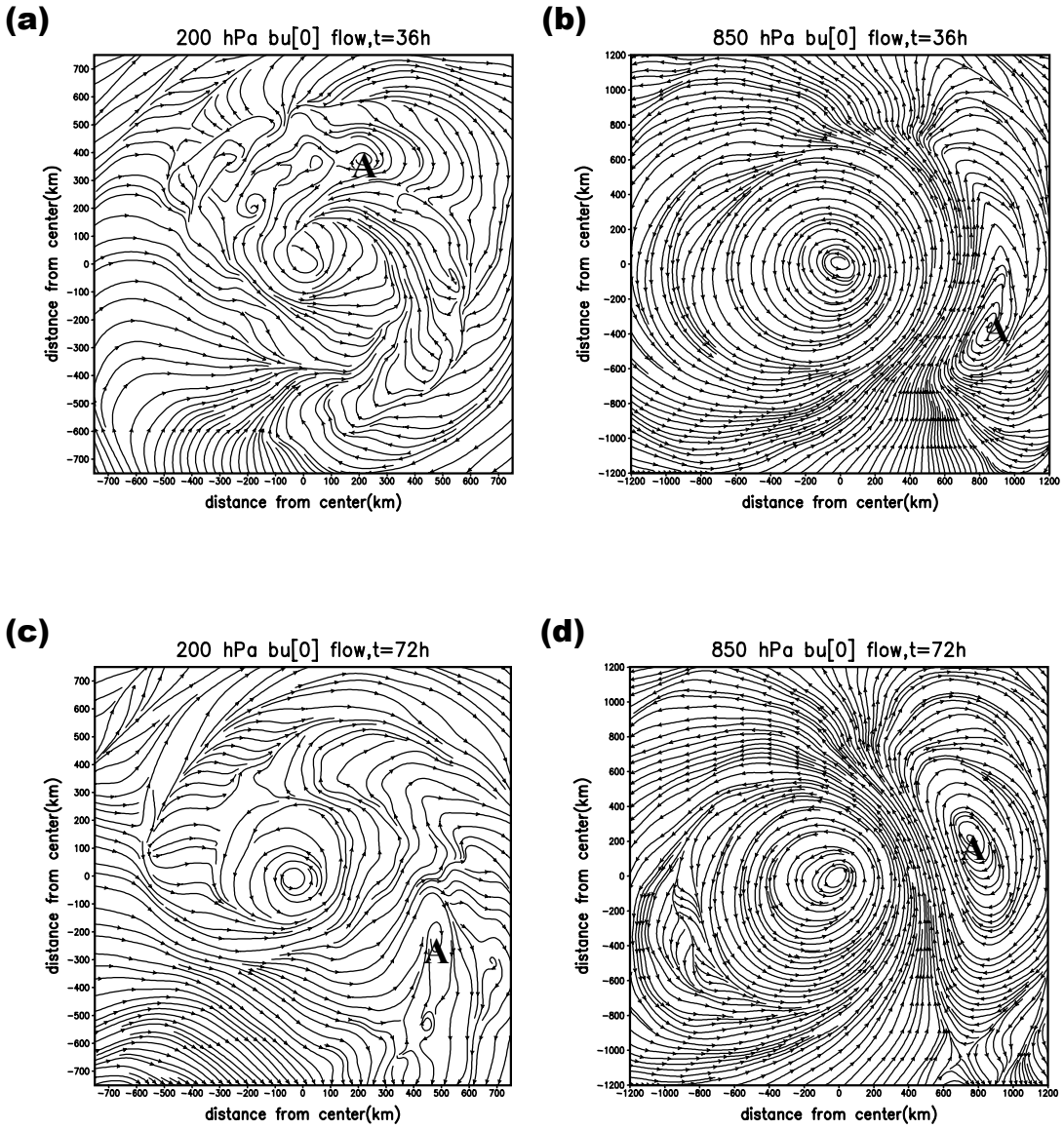

Fig. 9: As in Fig. 5 except for the bu[0] case.

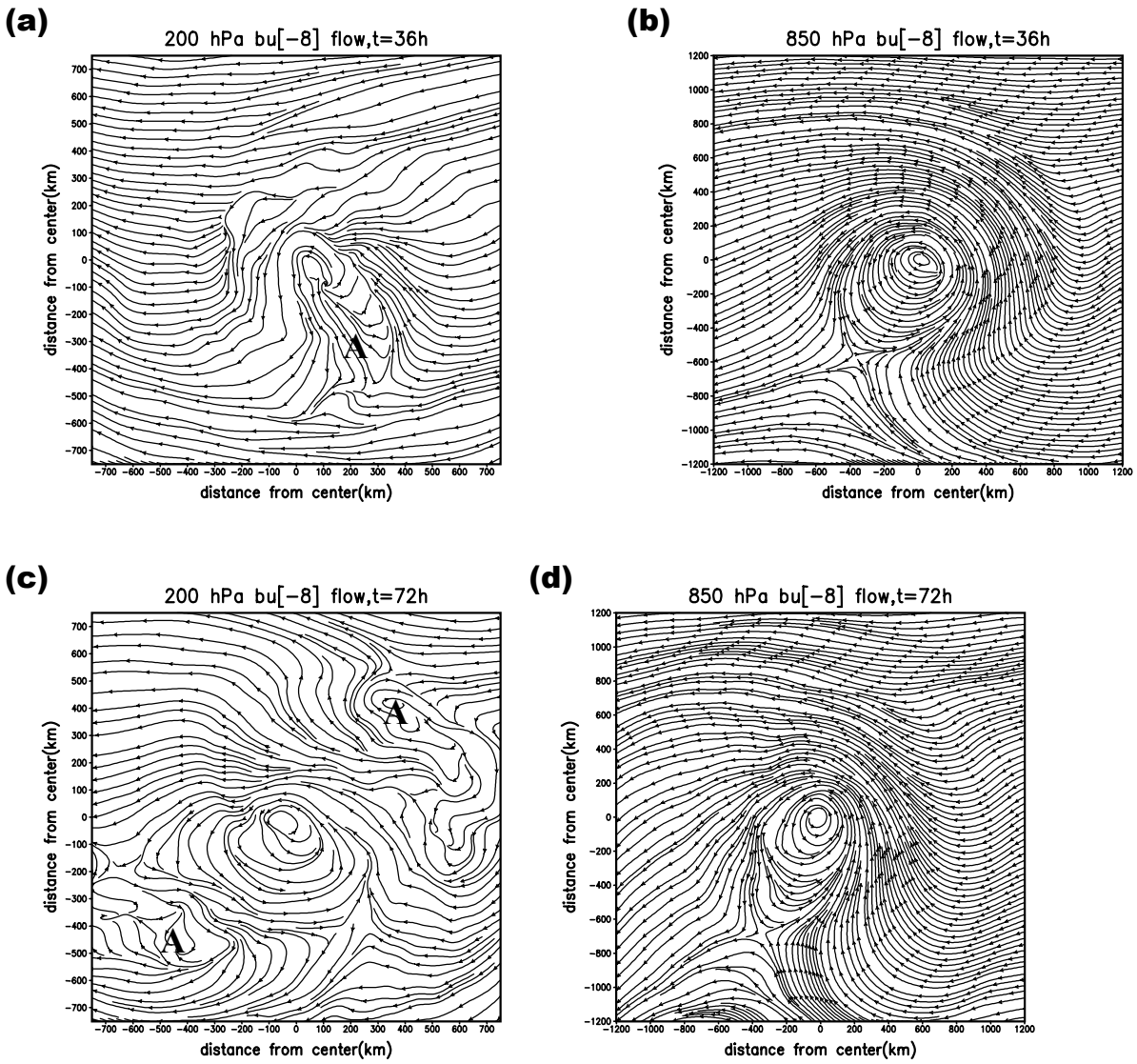

Fig. 10: As in Fig. 5 except for the bu[-8] case.

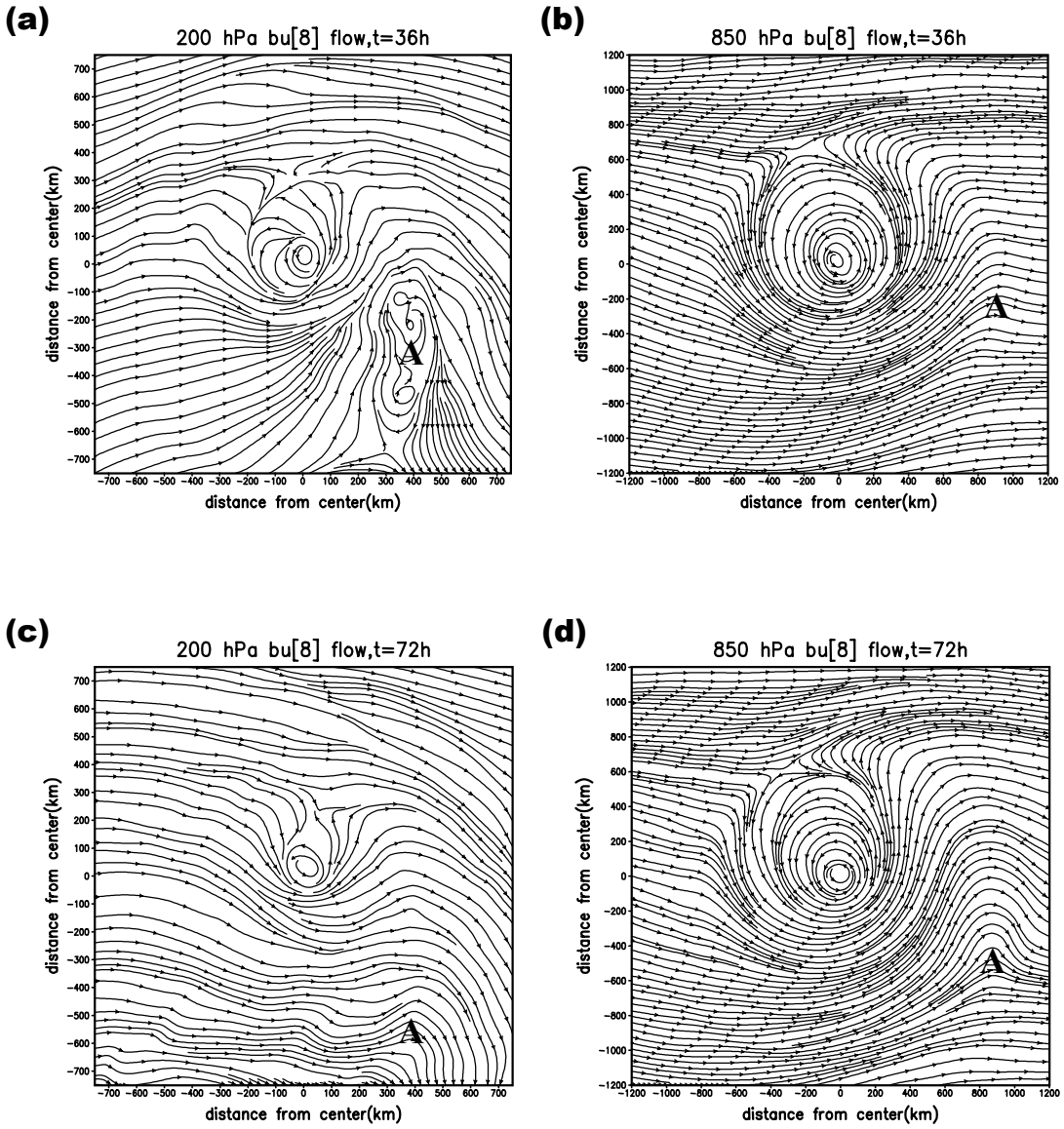

Fig. 11: As in Fig. 5 except for the bu[8] case.

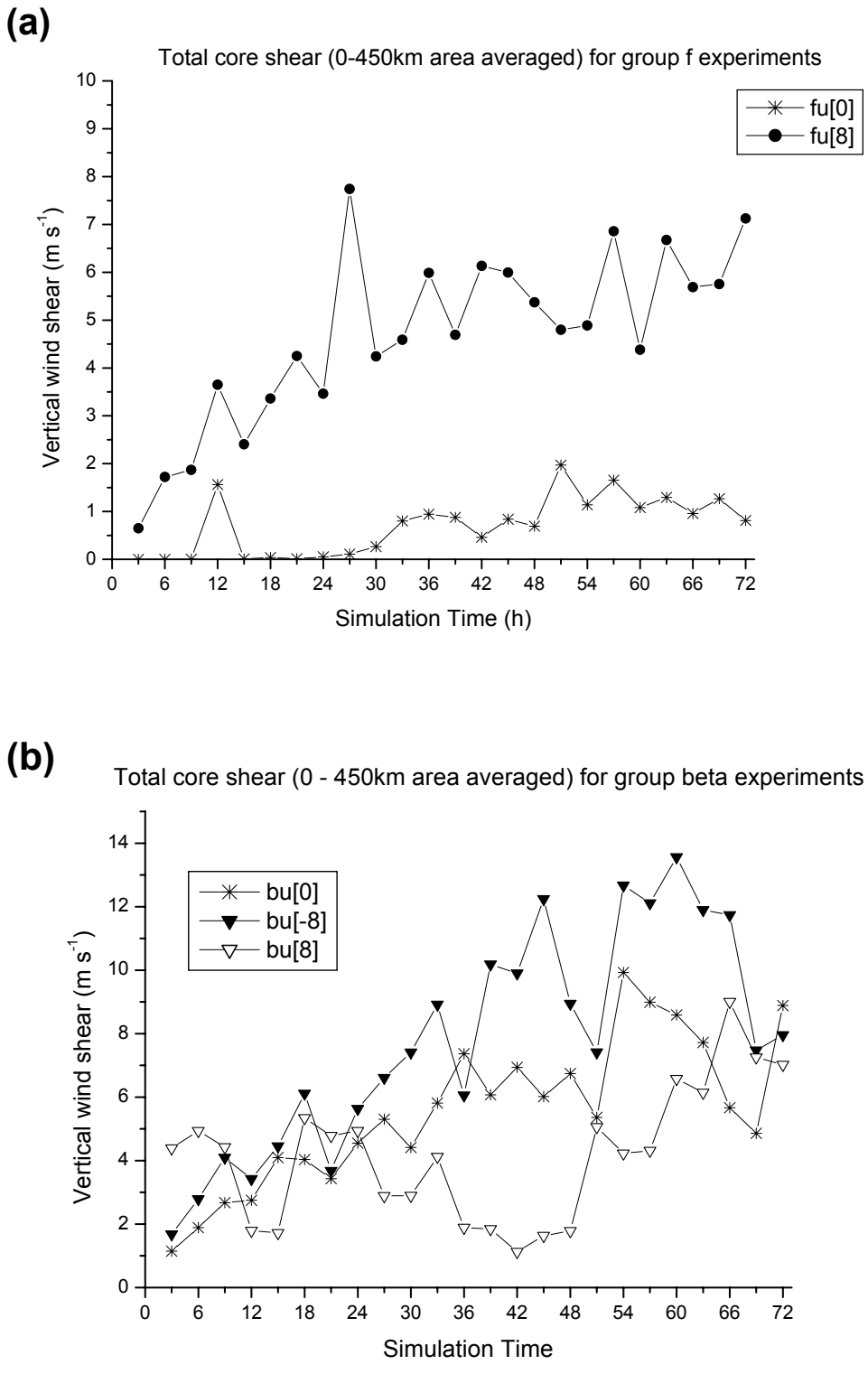

Fig. 12: Temporal variations of the 0 – 450 km area-averaged total vertical wind shear (200 - 850 hPa, unit: m s^{-1}) for (a) group f and (b) group beta experiments.

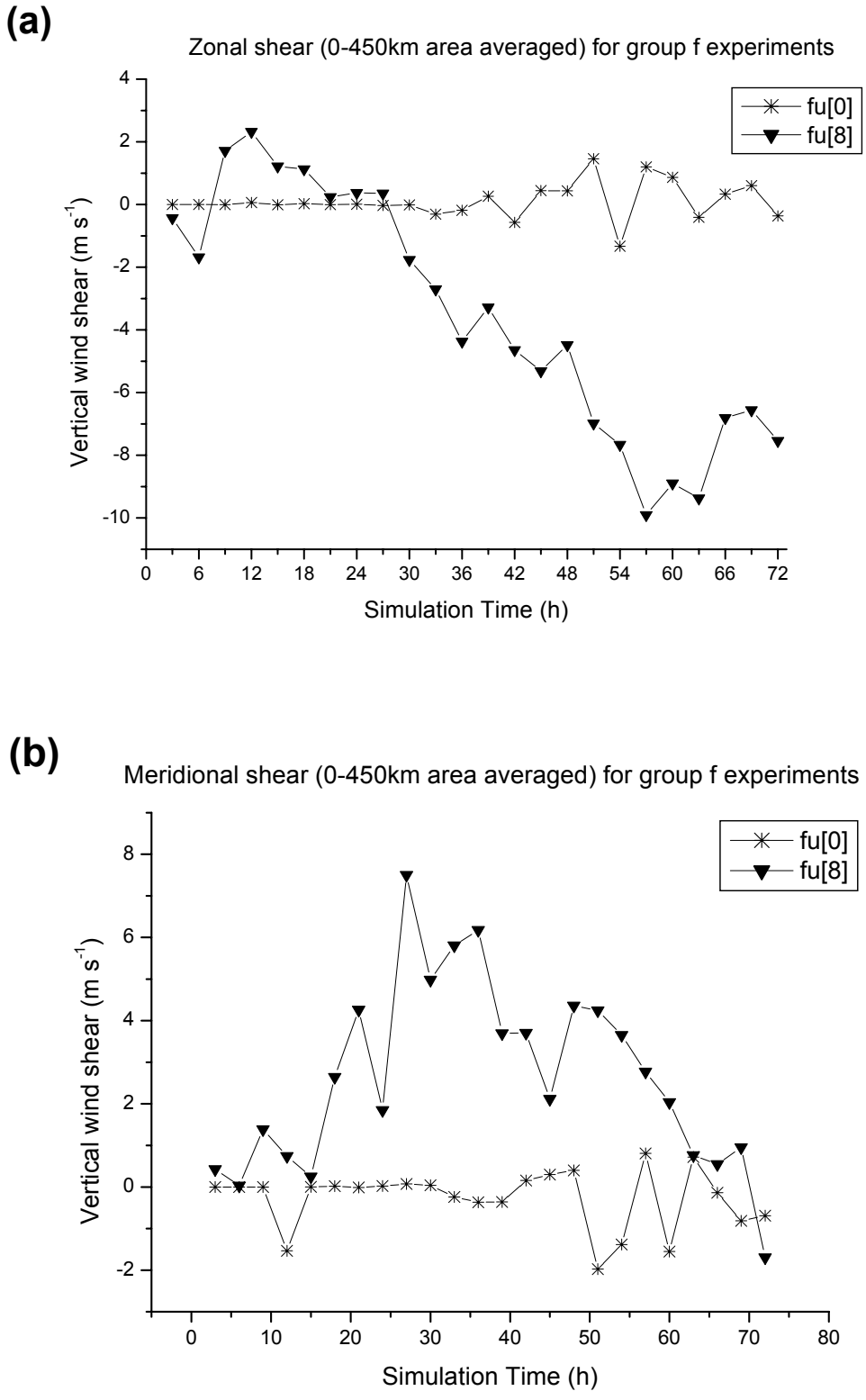

Fig. 13: 0 – 450 km area-averaged (a) zonal, (b) meridional vertical wind shear (200 - 850 hPa, unit: m s^{-1}) for group f experiments.

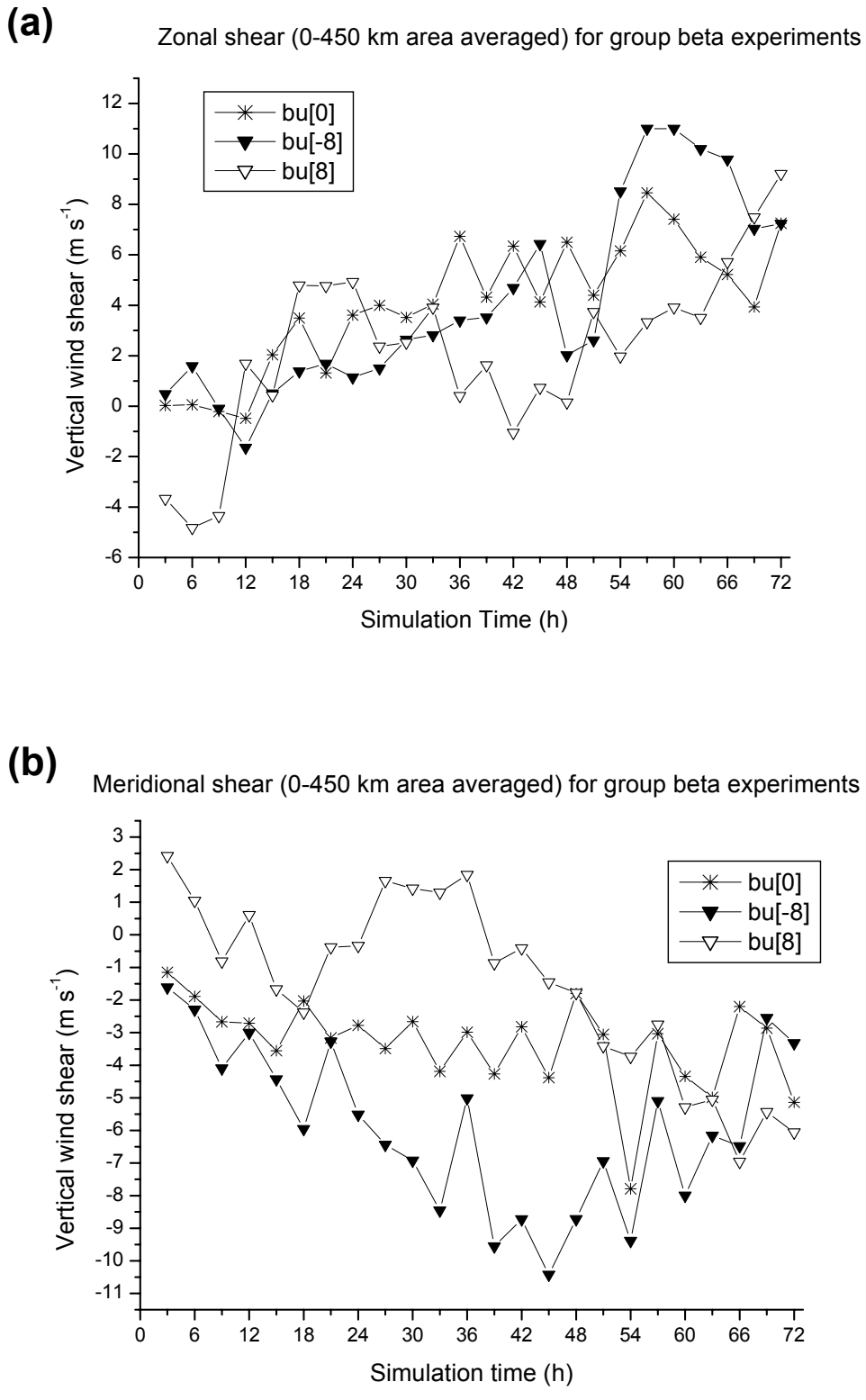

Fig. 14: As in Fig. 13 except for the group beta experiments.

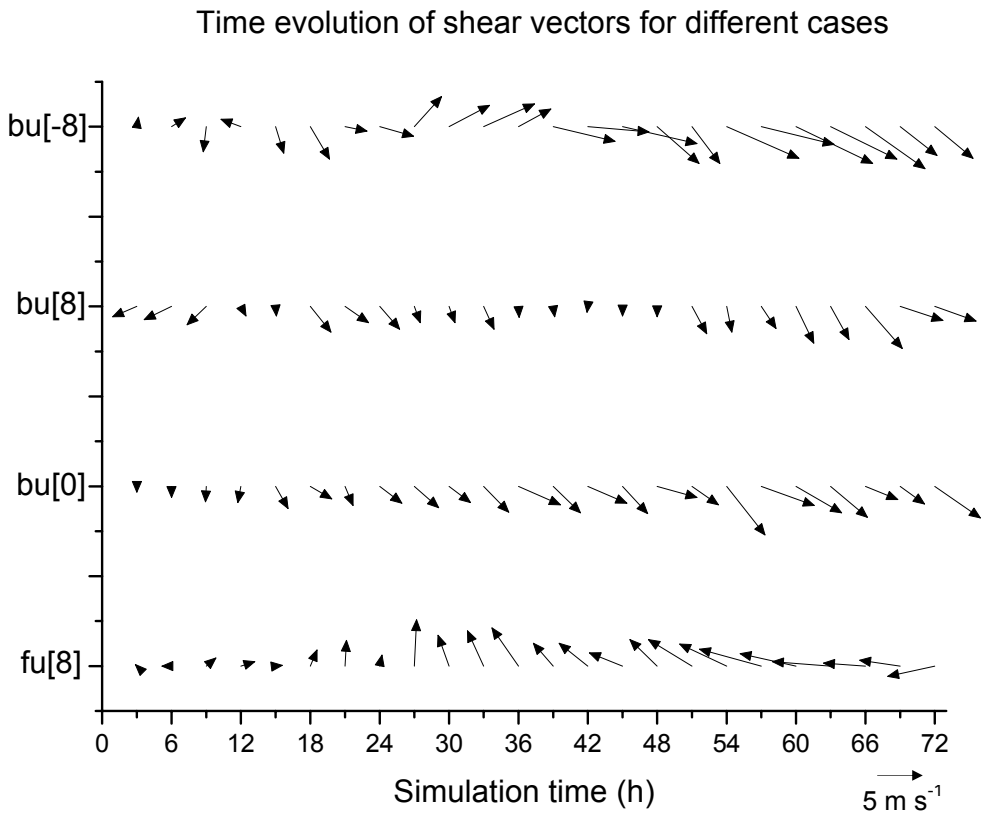

Fig. 15: Time evolution of the vector shear for the fu[8], bu[0], bu[8] and bu[-8] cases respectively.

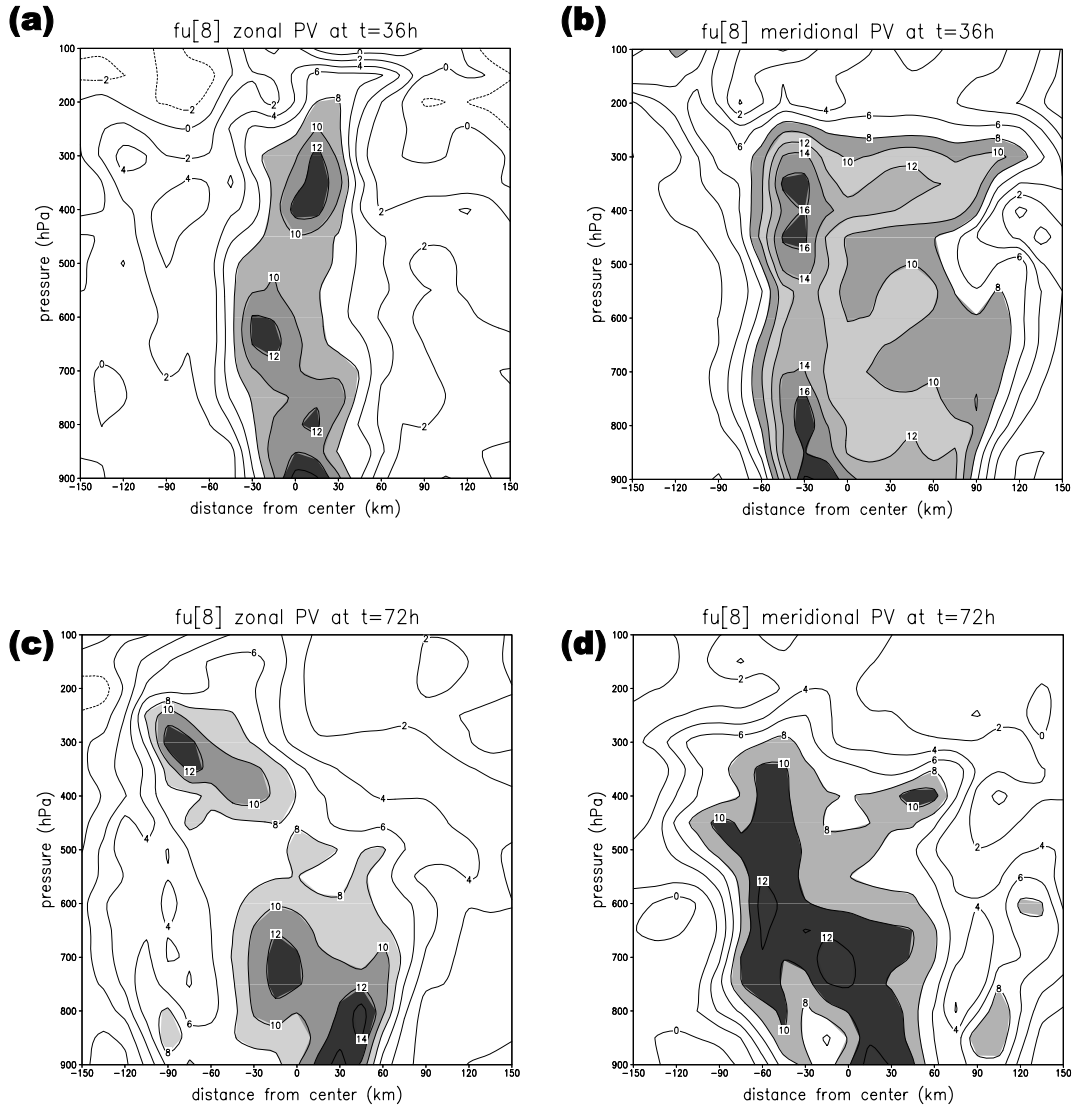

Fig. 16: Vertical potential vorticity variations (unit: PVU) in (a),(c) zonal component, and (b),(d) meridional component for the fu[8] case, values larger than 8 PVU are shaded. (Contour intervals: 2)

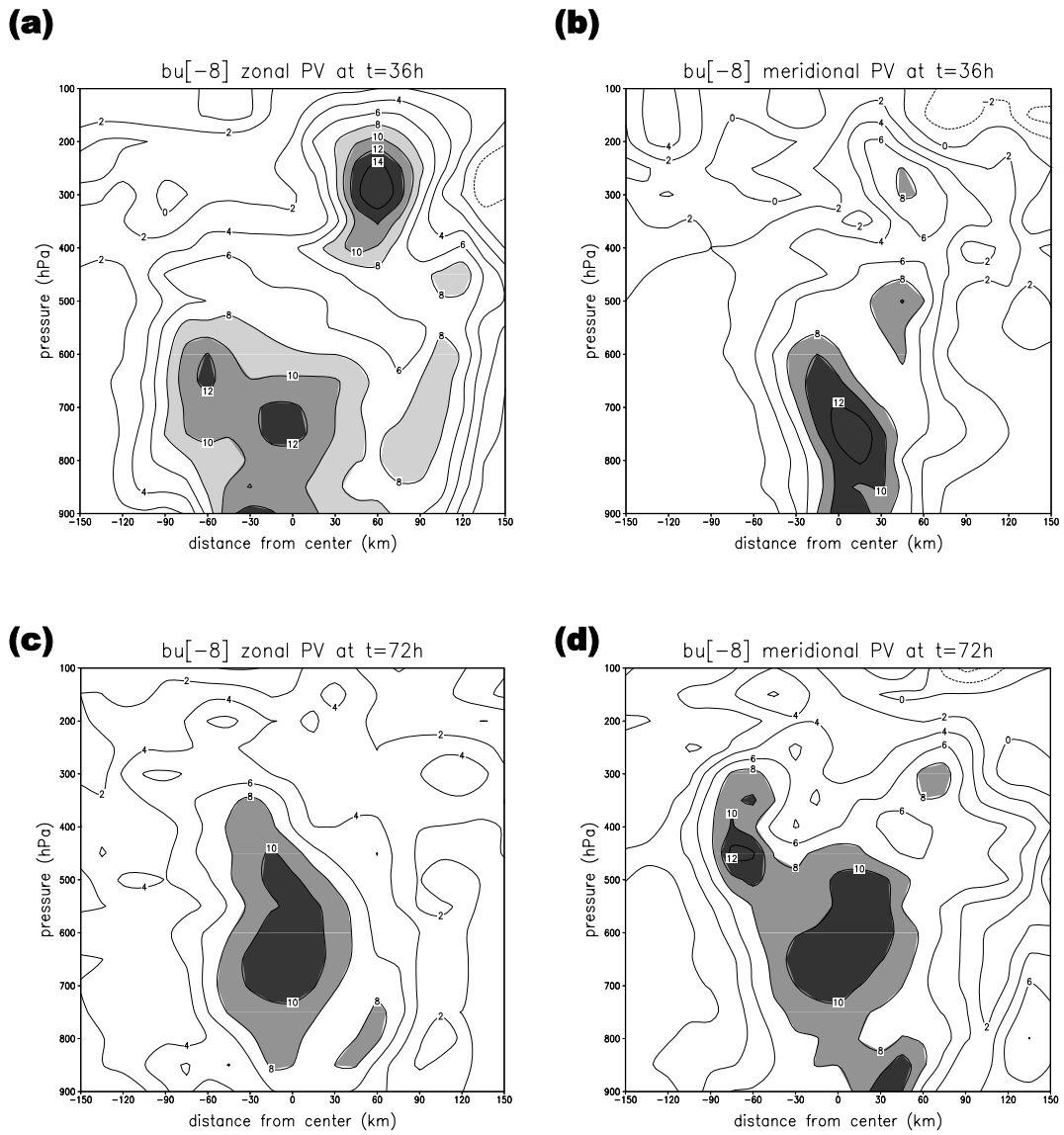

Fig. 17: As in Fig.16 except for the bu[-8] case.

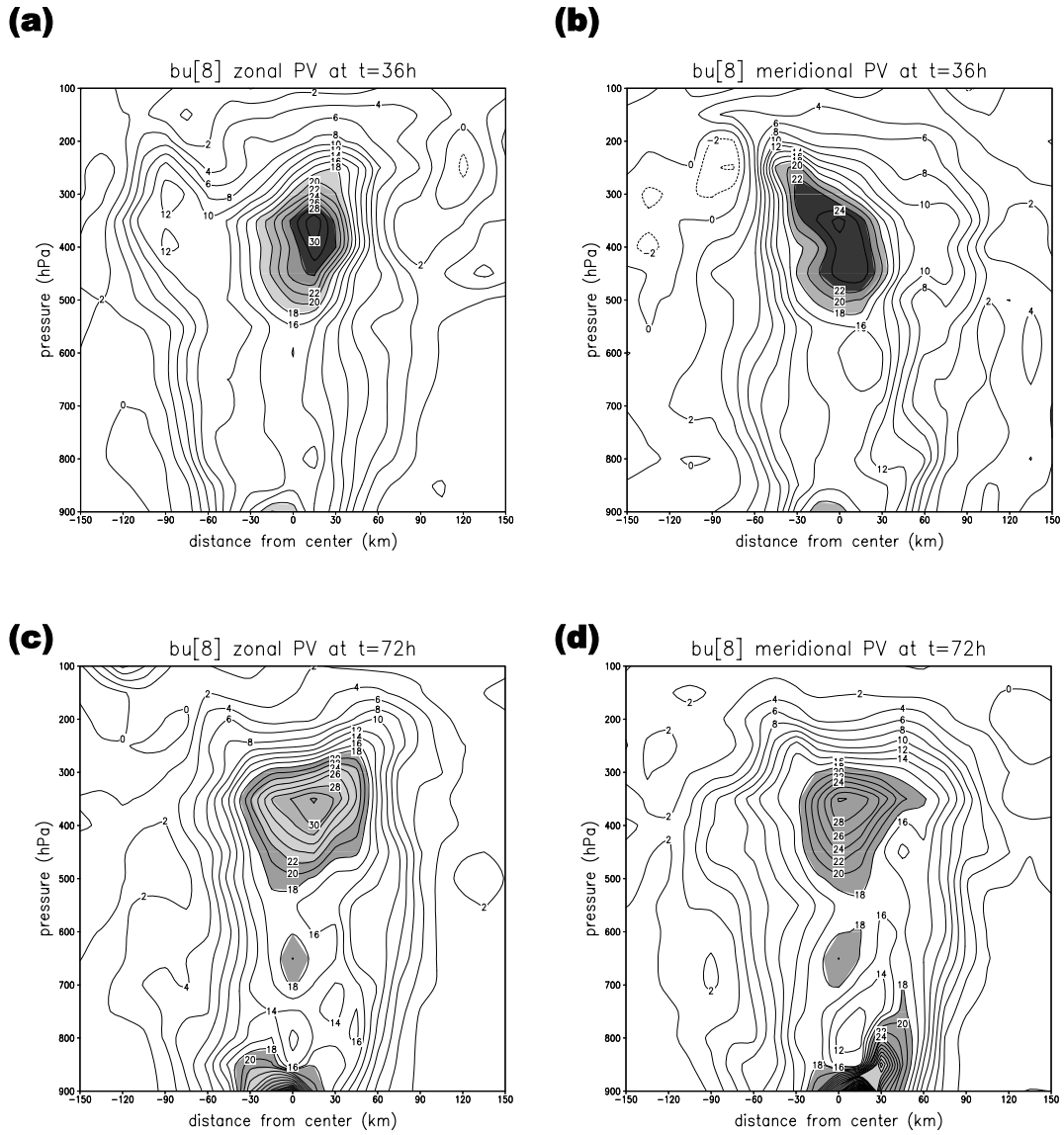

Fig. 18: As in Fig. 16 except for the bu[8] case, values larger than 18 PVU are shaded (contour interval: 2).

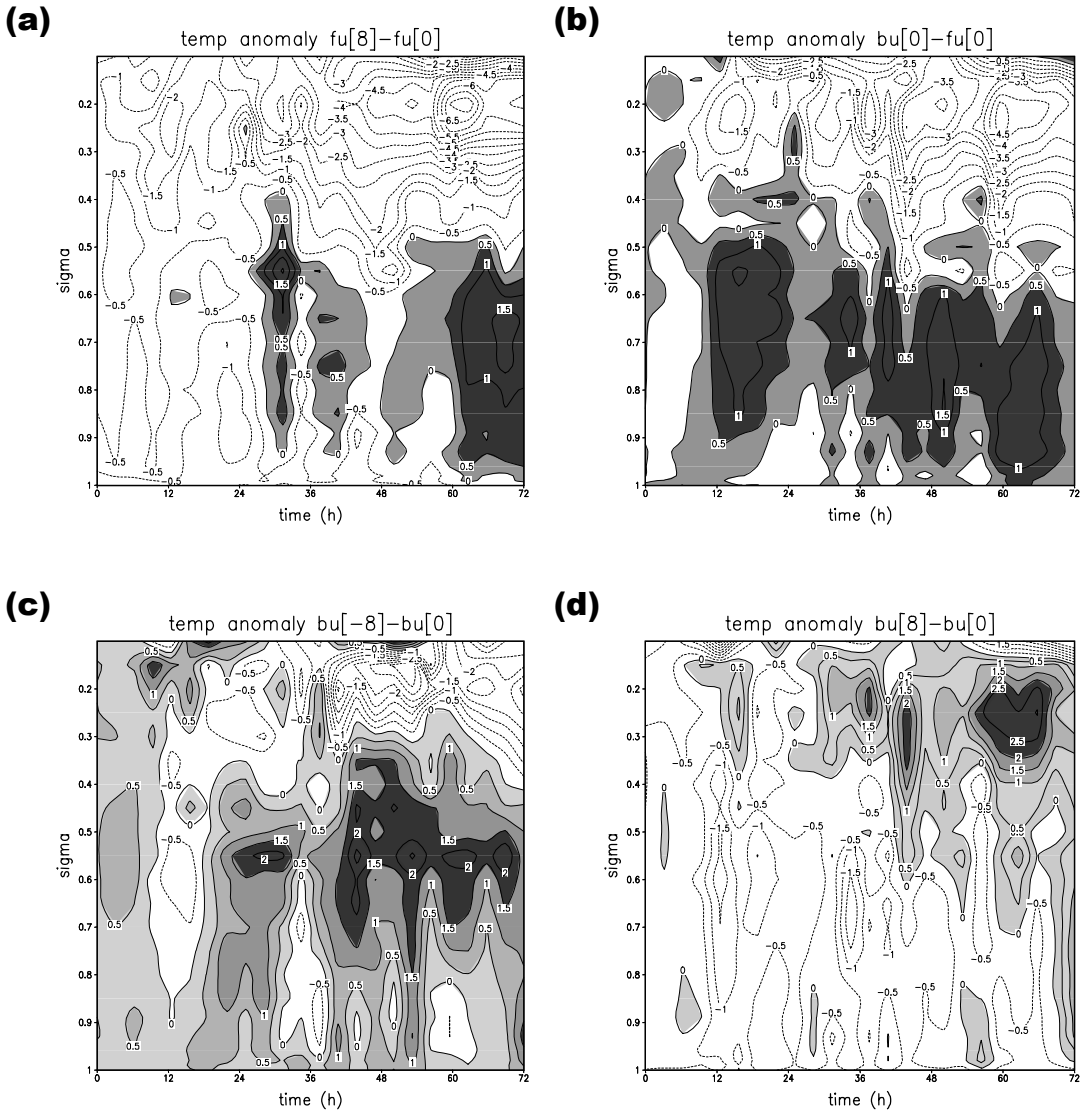

Fig. 19: Time-height cross-section of temperature anomalies with a radius of 60 km from the vortex center (unit: K) for (a) fu[8] and (b) bu[0] cases relative to that of fu[0], and (c) bu[-8], and (d) bu[8] cases relative to that of bu[0]. Positive values are shaded. (Contour interval: 0.5)

Table 1: The 9 experiments in 2 groups with different uniform flow speeds.

Uniform flow speed (m s^{-1})	Group f (constant *f*)	Group beta (variable *f*)
0	fu[0]	bu[0]
4	fu[4]	bu[4]
6	fu[6]	--
8	fu[8]	bu[8]
-4	--	bu[-4]
-8	--	bu[-8]